An Improved Method for the Expression and Purification of Porcine Dihydropyrimidine Dehydrogenase

Brett A. Beaupre, Joseph V. Roman and Graham R. Moran*

Department of Chemistry and Biochemistry, Loyola University Chicago, Flanner Hall, 1068 W Sheridan Rd, Chicago, IL 60660

*To whom correspondence should be addressed: Email: gmoran3@luc.edu, Ph: (414) 940 0059.

Abstract: Dihydropyrimidine dehydrogenase (DPD) catalyzes the reduction of uracil and thymine bases with electrons derived from NADPH. The mammalian DPD enzyme is a functional homodimer and has an elaborate cofactor arrangement. Two flavin cofactors (FAD and FMN) reside in two active site cavities that are separated by around 60 Å. The flavins are apparently bridged by four Fe_4S_4 clusters, two of which are provided by the partner protomer of the dimer. The study of DPD has been hampered by modest yield from both native sources and from heterologous expression in *E. coli*. In addition, minimal active enzyme is obtained when the DPD gene is fused to an N-terminal 6His-tag. This limitation has dictated the use of traditional purification methods that are made more challenging by apparent over-expression of truncated and/or non-active forms of DPD. Here we detail methods of expression and purification that result in a ~4-fold improvement in the yield of active porcine DPD when expressed in *E. coli* BL21 DE3 cells via the pET plasmid expression system. The addition of ferrous ions and sulfate during induction provide a small increase in purified active enzyme. However, the addition of FAD and FMN during cell lysis results in a substantial increase in activity that also reduces the relative proportion of non-active, high molecular weight protein contaminants. We also describe methods that permit correlation of the flavin content with the amount of active enzyme and thus permit simple, rapid quantitation and evaluation of purified DPD sample.

Introduction: The enzyme dihydropyrimidine dehydrogenase is a flavoprotein that catalyzes the reduction of the 5,6-vinylic bond of the pyrimidine bases thymine and uracil with electrons derived from NADPH (Scheme 1). The chemistry involves two successive net hydride transfer reactions. For flavoproteins this type of chemistry is typically accomplished via a ping-pong kinetic mechanism where two electrons donated from NADPH (or some other reductant) reside transiently on the flavin cofactor prior to acquisition and reduction of the second substrate. X-ray crystal structures of DPD have revealed an elaborate cofactor arrangement [1, 2]. Two active sites are observed that each have a non-covalently associated flavin cofactor; one with FAD and another with an FMN. In addition, four Fe_4S_4 centers appear to form a conduit that bridges the flavin cofactors (two of which originate from the opposing subunit). The available structures also indicate that the FAD interacts with NADP molecules and the FMN with pyrimidines. Mammalian DPDs form a functional head to head homodimer of two 113 KDa subunits with a ~10,800 $Å^2$ buried interface[2, 3].

There is considerable pharmacological interest in DPD as it is the primary mode of 5-fluorouracil (5FU) detoxification. 5FU is one of the most commonly prescribed chemotherapeutic agents and is used in the treatment of multiple common cancers [4-6]. The efficacy of 5FU results from that fact that it is ostensibly isosteric with uracil, and so is incorporated into nucleotides where it has the capacity to disrupt the functions of DNA and RNA. The majority of its toxicity, however, is a result of it being converted to 5-fluoro-2'-deoxyuridine-5'-monophosphate (5F-dUMP), a potent inhibitor of thymidylate synthase [7-9]. In the treatment of cancer 5FU is given in relatively large doses over extended periods. This approach is used as 5FU has a remarkably short pharmacokinetic lifetime ($t_{1/2}$ ~20 min) that is directly dependent on the activity of DPD [10, 11]. The net basal DPD activity within an individual varies over a 30-fold range, as such over dosing and under dosing are of significant concern in the achievement of optimum efficacy [12, 13]. It is not surprising that modulation of DPD activity by inhibition has been suggested as a means to level the playing field for patients receiving 5FU. To this end, 5-ethynyluracil (5EU) is a covalent inhibitor of DPD that has FDA approval for co-administration during chemotherapy [14-16].

Despite the curious structure and medical importance of DPD, mechanistic investigation has been hindered by the low yield of enzyme purified from mammalian tissue (1-17μg/g of tissue)[17-19] and from heterologous expression (~1-2 mg/L of culture)[20, 21]. Initially, DPD was purified from human, pig and sheep liver tissue using relatively laborious purification procedures. Recombinant expression of porcine DPD utilizing *E. coli* (DH5α) provided a ~100-fold increase in purified enzyme yield versus tissue-derived protocols [20]. Despite these advancements, heterologous expression and purification protocols did not provide DPD yields sufficient for extensive biophysical investigation. The protocol described in this study is an improved method for the expression, purification and quantitation of porcine DPD, a homolog that exhibits 93% identity to the human form of the enzyme and has been proven to be amenable to *in vitro* biophysical studies[1, 2, 18, 20, 22, 23]. Here we offer an improved expression and purification protocol that yields an approximately 4-fold increase on the amount of purified active enzyme.

Materials and Methods

Materials: Competent BL21 (DE3) cells were obtained from New England Biolabs. Tris(hydroxymethyl)aminomethane (Tris), dipotassium hydrogen phosphate (KPi), ethylenediaminetetraacetic acid (EDTA), oxidized nicotinamide adenine dinucleotide phosphate ($NADP^+$), ammonium sulfate, nitric acid, phenylmethanesulfonyl fluoride (PMSF), and the Miller formulation of lysogeny broth (LB) powder were purchased from Fisher Scientific. Dithiothreitol (DTT) and reduced nicotinamide adenine dinucleotide phosphate (NADPH) were purchased from RPI Research Products. The sodium salt of ampicillin and dextrose powder were purchased from Spectrum Chemical. Sodium sulfate, ascorbic acid, iron sulfate, sodium dodecyl sulfate (SDS), isopropyl β-D-1-thiogalactopyranoside (IPTG), riboflavin 5'-monophosphate (FMN), sodium hydroxide, 5-methyluracil (thymine), 5-ethynyluracil (5EU) and uracil (U) were obtained from Sigma-Millipore. Streptomycin sulfate powder was made by Gibco. Flavin adenine dinucleotide (FAD) was purchased from TCI biomedical. Glycine was obtained from Promega.

Expression and Purification Protocol: The gene for porcine dihydropyrimidine dehydrogenase (DPD) optimized for heterologous expression in *E. coli* was synthesized and then subcloned into the expression plasmids pET17b and pET28a between the Nde I and Xho I restriction sites by Genscript. The respective plasmids, pSsDPD and pSsDPD+, were transformed into *E. coli* BL21 (DE3) cells, plated onto LB agar containing 100 μg/mL ampicillin (pSsDPD) or 25 μg/mL kanamycin (pSsDPD+) and grown for 16 hours at 37 °C. An individual, isolated colony was then used to inoculate ~20 mL of LB broth with 100 μg/mL ampicillin (pSsDPD) or 25 μg/mL kanamycin (pSsDPD+) and cultured at 37 °C with agitation (220 rpm) until early log phase growth. Cell stock aliquots were stored at -80 °C after the addition of sterile glycerol to 20% v/v.

Cell stocks containing the pSsDPD plasmid were thawed and plated (100 μL/plate) onto LB agar, 100 μg/mL ampicillin and incubated for 18 hours at 37 °C. The cell lawn from two plates was suspended in ~20 mL of sterile LB broth and used to inoculate 1 L of LB broth culture, 100 μg/mL ampicillin, pre-warmed to 37 °C. Growth of the inoculum on solid media improves antibiotic selection and resuspension minimizes transfer of resistance enzymes that accumulate in broth and undermine selection in the expression culture. Cells were cultured at 37 °C with

agitation (220 rpm) and the optical density at 600 nm was monitored until mid-log phase (OD ~ 0.5). The temperature was then reduced (25, 28 or 30 ^{o}C) for one hour in the presence or absence of 100 µM iron sulfate and 1 mM sodium sulfate. DPD expression was induced by the addition of 100 µM IPTG and the period of expression was 20 hrs. All subsequent DPD purification steps were carried out at 4 ^{o}C. Cells were harvested by centrifugation (4,000 g for 30 min) and suspended in ~20 mL/L cold buffer A (30 mM Tris, 2 mM DTT, 1 mM EDTA pH = 8.0). Flavin cofactors were added or omitted (50 µM FAD and 50 µM FMN) and the cell slurry was transferred into a pre-cooled stainless-steel beaker. The cells were then lysed by two 4 min bursts of sonication at 50 W using a Branson 450 sonifier. Lysed cells were centrifuged at 10,000 g for 45 minutes to pellet cell debris and the supernatant was decanted into an ice-cold beaker. DPD was observed to precipitate between 35% and 55% ammonium sulfate saturation. The 35% and 55% ammonium sulfate pellets were each collected by centrifugation at 10,000 g for 20 minutes. The 35% pellet was discarded, the 55% pellet was re-suspended in cold buffer A and diluted until the conductivity of the solution was below 5 msec. The sample was loaded onto an ion exchange column (Bio Rad Macroprep High Q, 26 x 140 mm) that was pre-equilibrated in buffer A. The column was washed with 100 mL of buffer A and protein was eluted with a 400 mL gradient from 0 to 100% buffer B (30 mM Tris, 300 mM NaCl, 2 mM DTT, 1 mM EDTA pH = 8.0) from which 5 mL fractions were collected. Fractions containing DPD activity were pooled and concentrated to ~2 mL using a 10 KDa nominal molecular weight cutoff centrifugal concentrator (Millipore, Amicon). The concentrated sample was injected onto a 26 x 1000 mm Sephacryl S-200 High-Resolution size exclusion column (Pharmacia Biotech) and eluted with 300 mL of Buffer C (30 mM KPi, 2 mM DTT pH = 7.4). Fractions (5 mL each) were collected and those containing pure DPD were pooled, concentrated and frozen as aliquots at -80 ^{o}C. Subsamples from each stage of purification were taken and analyzed for purity using SDS PAGE and assayed for activity. To assess the enhancement of yield with the exogenous additives (FAD, FMN, iron sulfate, sodium sulfate), the above protocol was repeated without inclusion of these substances. Excluding the additives is representative of the DPD yield obtained by prior published methods [20-23].

For expression of DPD fused to an N-terminal 6His-tag, a 1 mL cell stock containing the pSsDPD+ plasmid was thawed and plated onto LB agar, 25 µg/mL kanamycin and incubated for

~18 hours at 37 °C. The lawn of cells obtained from two plates were suspended into ~20 mL sterile LB broth and transferred to pre-warmed LB broth cultures, 25 µg/mL kanamycin (2 plates/L) and grown at 37 °C with shaking (220 rpm) until and the optical density at 600 nm was 0.6. The temperature was then reduced to 30 °C for 1 hour prior to induction of DPD expression by the addition of IPTG to 100 µM. After ~18 hours of expression at 30 °C the cells were harvested, re-suspended in buffer D (30 mM KPi, 10 mM imidazole, 2 mM 2-mercaptoethanol pH 7.4) and sonicated as described above. The sonicate supernatant was loaded onto a HiTrap TALON affinity column equilibrated in buffer D. DPD was eluted with a 400 mL gradient from 10 to 300 mM imidazole in buffer D and 5 mL fractions were collected. The fractions that contained pure DPD were pooled and concentrated and stored as described above.

Activity Assay: Steady state activity assays were used to determine the units of activity specific to DPD. Crude or purified DPD (10-20 µL) was added to a quartz cuvette containing buffer E (30 mM KPi, 2 mM 2-mercaptoethanol, pH 7.4) and 200 µM NADPH. The reaction was monitored at 340 nm for the background oxidation of NADPH ($\Delta\varepsilon$ = 6,220 M^{-1} cm^{-1}) that arises via the activity of contaminant proteins and/or dioxygen reduction by DPD. After ~100 seconds, 100 µM uracil was added and the reaction was monitored for and additional 100 seconds. To obtain a measure of the activity specific to DPD, the background rate was subtracted from the rate observed in the presence of uracil.

Determinations of Cofactor Occupancy: FAD and FMN cofactor occupancy of DPD was assessed by diluting purified DPD into buffer D with the addition of 0.2 % SDS and 3 mM EDTA. EDTA was used to sequester the iron liberated from the Fe_4S_4 clusters by SDS induced denaturation of the enzyme, eliminating UV/Vis spectral contributions from the metal ions. The sample was then heated to 70 °C for 60 minutes to denature the enzyme and release the bound cofactors. Absorbance spectra (250 to 850 nm) were collected before the addition of 0.2% SDS and after heat denaturation. In order to remove the SDS from the sample, as required for HPLC analysis, samples were treated with KPi, pH 6.5 to 1 M, cooled to 4 °C and centrifuged for 15 minutes at 10,000 g. The supernatant (20 µL) was then injected onto a C18 column (XBridge C18, 5 µm, 4.6

x 250 mm) pre-equilibrated in 5 mM ammonium acetate with 15 % MeOH at pH 6.5. The sample was eluted isocratically at 1 mL/min and monitored at 370 nm. In order to prevent peak splitting due to multiple protonation states, FAD and FMN samples and standards were prepared in Buffer D at pH 6.5. This method allowed for baseline separation of FAD and FMN. To accurately quantify the FAD and FMN in the sample, a standard curve based on peak area was prepared for both compounds and the linear dependencies were used to determine the concentration of each of the flavins in the sample of DPD.

To determine the amount of iron in the DPD sample a method for quantifying iron using ferene-S was adopted from Hedayati et al., 2018 [24]. Ferene-S is a bidentate Fe(II) chelator and exhibits a large extinction coefficient change (ε_{595nm} = 35,194 M^{-1} cm^{-1}) when chelated to Fe(II) and thus can be used to accurately determine ferrous iron concentration [24, 25]. Briefly, 5-10 µL of DPD whose UV/Vis spectrum and flavin content was known, was treated with 100 µL of concentrated nitric acid for 90 minutes at 70 °C. The digested samples were cooled to 20 °C and neutralized with 160 µL of 10 N NaOH. A 740 µL solution of 5 mM ferene-S, 0.2 M ascorbic acid, 0.4 M ammonium acetate at pH 4.3 was added to the denatured DPD sample. The absorbance was measured after incubation for 15 hrs at 20 °C in the absence of light. All measurements were repeated with two separate preparations of DPD.

Determination of Active Enzyme: The proportion of active enzyme was assessed spectrophotometrically by reaction of DPD with NADPH and 5EU. 5EU will covalently cross-link to the C671 residue of DPD [26]. Three concentrations of DPD in buffer E were prepared anaerobically by adding concentrated enzyme to buffer that included 1 U/mL glucose oxidase and 1 mM dextrose that had been pre-sparged for 5 min with purified argon. This sample was then mounted onto a TgK stopped-flow spectrophotometer (Hitech Scientific). The sample was mixed with anaerobic NADPH (400 µM) and 5EU (400 µM), also prepared by sparging with argon. The reaction was monitored for the oxidation of NADPH at 340 nm. The absorbance change at 340 nm was quantified using the known extinction coefficient for NADPH oxidation (6,220 $M^{-1}cm^{-1}$). The data obtained were fit to equation 1 which describes an exponential added to a straight line. In this equation ΔA_{340} is the change in absorbance at 340 nm during the exponential phase

and m is the slope of the linear portion of the curve that occurs due to adventitious reduction of DPD and C is the endpoint of exponential phase.

Equation 1 $$A_{340} = \Delta A_{340}(e^{-k_1 t}) + mt + C$$

Results

Expression and Purification: Expression and purification of DPD using the method described above yields ~14 units of activity from 10 liters of culture. The UV/Vis absorption maxima of the purified enzyme were 280, 380 and 426 nm in a 3.6:1.1:1 intensity ratio. The absorption spectrum of DPD is a composite of two flavin spectra and four Fe_4S_4 clusters. Purified enzyme was stable in buffer E indefinitely when concentrated (>500 µM) and frozen at -80 °C. Activity and purity were assessed at each stage of purification. In Table 1 it is apparent that full length DPD is amenable to mechanical processing as ~60% of the activity observed at sonication is retained in the purified sample. The SDS-PAGE shown with Table 1 depicts the protein content of subsamples taken throughout purification. This gel indicates that the protocol yields ostensibly pure protein.

The addition of sodium sulfate and iron sulfate during expression resulted in only a small increase in yield (~0.1 unit of activity/L) suggesting that these substances are not significantly limiting in LB broth. However, the combined addition of sulfate and iron during expression in addition to FAD and FMN at the point of sonication resulted in a net gain of ~1 unit of activity per liter of culture which equates to a 3.5-fold increase in total activity recovered. Expression of the 6His-tag-DPD from the pSsDPD+ construct in the manner described above resulted in ~30% (<0.1 unit/L) of the activity observed with the native length protein in the absence of additives, nullifying any advantage of the purification tag. Low yields of N-terminal 6His fusion DPD have been reported in two prior studies [12, 21] who also describe sub-milligram yields per liter of culture. While the stability and tractability of this form of the enzyme was not evaluated, the His-tagged enzyme had ostensibly identical absorption characteristics to those of the purified wild-type enzyme.

Figure 1 summarizes the chromatographic purification of SsDPD. Figure 1A & B show purity of the fractions containing DPD as eluted from Q-sepharose and SEC columns respectively. DPD was identified as the uppermost band on the SDS PAGE gel and runs at ~115KDa.

Figure 1C & D depict activity of DPD purified by the current method and chromatograms for the prior and current methodologies. The Q-sepharose data (Figure 1A &C) indicate that the DPD protein co-expresses with at least three additional proteins that are not observed to accumulate in non-induced controls (data not shown). Presumably, these are truncated and/or partially apo-

forms of DPD. However, the identity of these species was not established in the current study. The uracil specific activity correlates only with the first eluting form that is also the dominant component (solid line). Though not shown, all fractions have significant long wavelength spectral characteristics indicative of Fe-S centers. Pooling only the active fractions from Q-sepharose eliminates the greatest part of apparent contaminant protein components. In Figure 1C the enhancement achieved by the addition of Fe(II) and sulfate and the combined addition of Fe(II), sulfate and flavins can be observed. The amount of active DPD eluting based on 280 nm absorption is increased by a factor of 2.42 by the addition of flavins. Figure 1B & D summarizes the SEC chromatographic step. These data indicate that the bulk of the DPD activity is associated with the first eluting fraction and that most impurities elute afterward. Similarly, in Figure 1D we see the gain in total DPD yield achieved by the Fe(II), sulfate and flavin additives (solid line).

Determination of Fraction of Active Enzyme*:* The proportion of active enzyme as a function of absorption was determined by titrating known amounts of DPD with excess 5EU in the presence of NADPH. It has been established that 5EU inhibits DPD by forming a covalent link with cysteine 671 that is the putative active site acid facilitating hydride transfer from $FMNH_2$ to pyrimidine substrates [21, 26]. In the presence of excess NADPH and 5EU, DPD will consume an amount of NADPH equal to the DPD•5EU complex in an initial and relatively rapid exponential phase. Adventitious slow reduction of the enzyme follows this initial exponential phase. The data were fit to an exponential term added to a straight line to obtain the amplitude of the exponential portion of the curve (Equation 1). The amplitude of this phase at 340 nm represents the 5EU-dependent oxidation of NADPH to $NADP^+$ (6,220 $M^{-1}cm^{-1}$) and can be reasonably regarded as a measure of the concentration of active DPD in the assay. The amplitude of this phase was plotted versus the absorbance of DPD in the sample where the linear dependence represents the concentration of DPD as a function of absorbance at 426 nm (Figure 2A). The slope of the line of best fit is thus the 426 nm DPD extinction coefficient (76,600 $M^{-1}cm^{-1}$). The concentration of active enzyme correlated with the concentration of enzyme bound flavins (FAD and FMN) indicating that the isolated enzyme is, within error, fully active.

***Determination of the Cofactor Occupancy*:** HPLC analysis of denatured DPD was used to quantify FAD and FMN concentration by comparing the integrated area of the cofactor peaks to standard curves (Figure 3A & B). The denatured sample contained 19.8 ± 0.87 µM FAD and 20.9 ± 1.7 µM FMN. Comparison to active enzyme as described above indicates that the purified enzyme has within error a 1:1:1 ratio for FAD:FMN:active DPD. This ratio confirms that the purification protocol is selective for active holoenzyme.

The concentration of Fe(II) in the DPD protein was determined by a ferene-S assay and found to be 15.1-fold higher than that of either flavin, consistent with the 16-fold expected. The ferene-S•Fe(II) complex has longer wavelength absorption transitions than FAD or FMN and therefore the 595 nm absorbance value measured can be attributed entirely to this complex. From the above data we can conclude that the DPD sample as isolated is constituted almost exclusively with active enzyme. That the concentration of the flavins is equivalent and occur at the correct ratio with respect to Fe(II), permits the concentration of the enzyme to be determined solely by SDS denaturation in the presence of EDTA (Figure 3A). The combined extinction coefficient for FAD and FMN (23,500 $M^{-1}cm^{-1}$) can then be used to determine the active enzyme concentration. The extinction coefficient spectrum of DPD was generated by normalizing a DPD sample of known absorbance before and after denaturation (0.2% SDS, 3mM EDTA at 70 °C for 1 hour) to the amount of FAD and FMN in the sample (Figure 3). The normalize DPD absorbance spectrum was used to separately determine working extinction coefficients of 275,000 $M^{-1}cm^{-1}$, 82,282 $M^{-1}cm^{-1}$ and 74,220 $M^{-1}cm^{-1}$ at 280, 380 and 426 nm respectively (Figure 2) the latter of which agrees well with that derived from the 5EU based kinetic method above. The measured 426 nm extinction coefficient agrees well with prior reports that based this number on indirect methods such as Bradford assay [22, 27, 28].

Assuming minimal perturbation of the flavin spectra when bound to DPD, the difference spectrum obtained when the denatured (flavin only) spectrum was subtracted from the initial non-denatured spectrum resulted in a calculated extinction coefficient of 58,448 $M^{-1}cm^{-1}$ at 400 nm for the four Fe_4S_4 centers contained in one protomeric unit (Figure 3A). This indicates that the individual Fe_4S_4 centers contribute an average of ~14,600 $M^{-1}cm^{-1}$ to the DPD spectrum at

this wavelength. Such an absorption contribution is comparable to that of Fe_4S_4 centers observed in other systems [29, 30].

Discussion

The poor abundance from native sources, limited expression of recombinant DPD and the inability to quantify the amount of active enzyme present has led to a ~9-fold variation in published turnover numbers based on different enzyme extinction coefficients ranging from ~31,000 to 74,000 $M^{-1}cm^{-1}$ [3, 20-23, 31]. Here we present a ~4-fold improvement on the yield of active recombinant porcine DPD. The method not only improves the overall quantity obtained but also is shown to isolate only the active form of the enzyme from contaminants. The DPD isolated by these methods is shown to have near 100% cofactor loading and full activity.

Initial DPD preparations followed a modified method adapted from Lohkamp et al., 2010 and yielded ~0.3 units/L of DPD with inconsistent total activity and multiple contaminants as observed by SDS PAGE (data not shown) [21]. In order to optimize expression of DPD additives during expression and purification were assessed. Though not mentioned above, PMSF was added to assess the possibility that the protein of similar and lower mass observed to purify with full length DPD was or was not a product of proteolysis (Figure 1). It was determined that PMSF had no effect on purity or yields of active DPD which suggest that serine proteases are not responsible for the production lower molecular weight co-purifying proteins. Moreover, the use of BL21 (DE3) cells which are deficient in both OmpT (outer membrane) and Lon (cytoplasmic) protease systems as well as the inclusion of EDTA in the lysis buffer, apparently provides sufficient protection from proteolysis to permit purification of DPD over a three-day period. In addition, we observed that the use of streptomycin sulfate as an initial step to precipitate nucleic acids results in the precipitation and/or inactivation of DPD.

It is generally accepted that iron-sulfur clusters are unstable in the presence of dioxygen to the extent that many iron-sulfur protein purification protocols must be accomplished under anaerobic conditions [32, 33]. The resilience of DPD activity in atmosphere indicates that the Fe_4S_4 centers are sequestered within the protein are not susceptible to oxidative degradation. To assess if iron sulfur cluster generation was the limiting factor in DPD heterologous expression we added Fe(II) and sulfate to culture media in order to take advantage of *E. coli* cell transporters that uptake both exogenous iron and sulfate [34, 35]. The inclusion of these additives had a modest effect on yield, improving total activity by ~25% (Table 1). DPD isolated with the addition

of Fe(II) and sulfate had a spectrum with increased relative long-wavelength absorption particularly around 400 nm which is maximal for the Fe_4S_4 centers (Figure 3 & 4).

Supplementation of FAD and FMN during sonication resulted in a ~4-fold increase in total activity yield. However, supplementation of flavins to purified enzyme did not show a rate enhancement (data not shown) and largely suggests that the purified, active enzyme is devoid of partially or fully apo-enzyme with respect to flavins. The effect of added flavins during purification can be seen in the 280 nm normalized spectra that compare DPD purified by the three methods assessed (Figure 4).

The additive spectra show a decrease in the 280:426 nm absorption ratio, indicating that the enzyme isolated with Fe(II), sulfate and flavins has a higher degree of cofactor incorporation. However, the increase does not by itself account for the 4-fold increase in total activity that the additives provide. This suggests that the original method copurified some fraction of partially or fully apo-enzyme and that the principle advantage observed with the addition of flavins during lysis is a result of incorporation of flavins to this form of the enzyme which results in more of the expressed DPD protein purifying as the active component (Figure 4).

An active DPD protomer requires one FAD, one FMN, and four Fe_4S_4 centers for catalytic activity. Interestingly, data from this study suggests that FAD and FMN are present in purified denatured DPD samples in a 1:1 ratio, an observation supported by other investigators [20-22, 36]. This observation suggests that the apo, mono- and di-flavin bound DPD forms are separated during purification given that the contingent binding of flavins is a less likely cause of this ratio. These data correlate directly to the amount of active enzyme determined by 5EU titration and the calculated extinction coefficients from denaturation experiments. Based on this the active amount of DPD can be accurately assessed by either titration to 5EU or using the calculated net extinction coefficient for bound flavin cofactors.

Conclusion

A longstanding difficulty encountered by DPD researchers was the inability to prepare the enzyme in quantities amenable to transient state kinetic analyses. This was exacerbated by limited expression of a N-terminal 6His-tagged variant dictating the use of traditional purification methods which involve multiple additional steps. These additional steps add considerable time to the protocol which is an added restriction to biophysical investigations. These limitations highlight the need for an improved method of expression and purification. The modifications to the protocol described here result in an approximately 4-fold increase in active DPD yield and the quantitation methods described provide means for simple, rapid and accurate assessment of the proportion of active DPD in the sample obtained.

References

[1] D. Dobritzsch, G. Schneider, K.D. Schnackerz, Y. Lindqvist, Crystal structure of dihydropyrimidine dehydrogenase, a major determinant of the pharmacokinetics of the anti-cancer drug 5-fluorouracil. EMBO J 20 (2001) 650-660.
[2] D. Dobritzsch, S. Ricagno, G. Schneider, K.D. Schnackerz, Y. Lindqvist, Crystal structure of the productive ternary complex of dihydropyrimidine dehydrogenase with NADPH and 5-iodouracil. Implications for mechanism of inhibition and electron transfer. J Biol Chem 277 (2002) 13155-13166.
[3] D. Dobritzsch, K. Persson, G. Schneider, Y. Lindqvist, Crystallization and preliminary X-ray study of pig liver dihydropyrimidine dehydrogenase. Acta Crystallogr D Biol Crystallogr 57 (2001) 153-155.
[4] D.B. Longley, D.P. Harkin, P.G. Johnston, 5-fluorouracil: mechanisms of action and clinical strategies. Nat Rev Cancer 3 (2003) 330-338.
[5] B. Tallon, N. Turnbull, 5% fluorouracil chemowraps in the management of widespread lower leg solar keratoses and squamous cell carcinoma. Australas J Dermatol 54 (2013) 313-316.
[6] A. Gangjee, H.D. Jain, S. Kurup, Recent advances in classical and non-classical antifolates as antitumor and antiopportunistic infection agents: Part II. Anticancer Agents Med Chem 8 (2008) 205-231.
[7] C. Heidelberger, Biochemical Mechanisms of Action of Fluorinated Pyrimidines. Exp Cell Res 24 (1963) SUPPL9:462-471.
[8] R.J. Kent, C. Heidelberger, Fluorinated pyrimidines. XL. The reduction of 5-fluorouridine 5'-diphosphate by ribonucleotide reductase. Mol Pharmacol 8 (1972) 465-475.
[9] R.T. Reilly, K.W. Barbour, R.B. Dunlap, F.G. Berger, Biphasic binding of 5-fluoro-2'-deoxyuridylate to human thymidylate synthase. Mol Pharmacol 48 (1995) 72-79.
[10] G. Milano, M.C. Etienne, Dihydropyrimidine dehydrogenase (DPD) and clinical pharmacology of 5-fluorouracil (review). Anticancer Res 14 (1994) 2295-2297.
[11] G.D. Heggie, J.P. Sommadossi, D.S. Cross, W.J. Huster, R.B. Diasio, Clinical pharmacokinetics of 5-fluorouracil and its metabolites in plasma, urine, and bile. Cancer Res 47 (1987) 2203-2206.
[12] K. Ogura, T. Ohnuma, Y. Minamide, A. Mizuno, T. Nishiyama, S. Nagashima, M. Kanamaru, A. Hiratsuka, T. Watabe, T. Uematsu, Dihydropyrimidine dehydrogenase activity in 150 healthy Japanese volunteers and identification of novel mutations. Clin Cancer Res 11 (2005) 5104-5111.
[13] R.B. Diasio, M.R. Johnson, Dihydropyrimidine dehydrogenase: its role in 5-fluorouracil clinical toxicity and tumor resistance. Clin Cancer Res 5 (1999) 2672-2673.
[14] T. Skovsgaard, N.G. Davidson, M.J. Piccart, D.J. Richel, J. Bonneterre, D.T. Cirkel, C.M. Barton, G. Eniluracil/Fluorouracil Breast Cancer Study, A phase II study of oral eniluracil/fluorouracil in patients with anthracycline-refractory or anthracycline- and taxane-refractory advanced breast cancer. Ann Oncol 12 (2001) 1255-1257.
[15] B.G. Czito, T.J. Hong, D.P. Cohen, D.S. Tyler, C.G. Lee, M.S. Anscher, K.A. Ludwig, H.F. Seigler, C. Mantyh, M.A. Morse, A.C. Lockhart, W.P. Petros, W. Honeycutt, N.L. Spector, P.J. Ertel, S.G. Mangum, H.I. Hurwitz, A Phase I trial of preoperative eniluracil plus 5-fluorouracil and

radiation for locally advanced or unresectable adenocarcinoma of the rectum and colon. Int J Radiat Oncol Biol Phys 58 (2004) 779-785.
[16] E. Rivera, J.C. Chang, V. Semiglazov, O. Burdaeva, M.G. Kirby, T. Spector, Eniluracil plus 5-fluorouracil and leucovorin: treatment for metastatic breast cancer patients in whom capecitabine treatment rapidly failed. Clin Breast Cancer 14 (2014) 26-30.
[17] Y. Camadan, H. Ozdemir, I. Gulcin, Purification and characterization of dihydropyrimidine dehydrogenase enzyme from sheep liver and determination of the effects of some anaesthetic and antidepressant drugs on the enzyme activity. J Enzyme Inhib Med Chem 31 (2016) 1335-1341.
[18] B. Podschun, G. Wahler, K.D. Schnackerz, Purification and characterization of dihydropyrimidine dehydrogenase from pig liver. Eur J Biochem 185 (1989) 219-224.
[19] Z.H. Lu, R. Zhang, R.B. Diasio, Purification and characterization of dihydropyrimidine dehydrogenase from human liver. J Biol Chem 267 (1992) 17102-17109.
[20] K. Rosenbaum, B. Schaffrath, W.R. Hagen, K. Jahnke, F.J. Gonzalez, P.F. Cook, K.D. Schnackerz, Purification, characterization, and kinetics of porcine recombinant dihydropyrimidine dehydrogenase. Protein Expr Purif 10 (1997) 185-191.
[21] B. Lohkamp, N. Voevodskaya, Y. Lindqvist, D. Dobritzsch, Insights into the mechanism of dihydropyrimidine dehydrogenase from site-directed mutagenesis targeting the active site loop and redox cofactor coordination. Biochim Biophys Acta 1804 (2010) 2198-2206.
[22] K. Rosenbaum, K. Jahnke, B. Curti, W.R. Hagen, K.D. Schnackerz, M.A. Vanoni, Porcine recombinant dihydropyrimidine dehydrogenase: comparison of the spectroscopic and catalytic properties of the wild-type and C671A mutant enzymes. Biochemistry 37 (1998) 17598-17609.
[23] K. Rosenbaum, K. Jahnke, K.D. Schnackerz, P.F. Cook, Secondary tritium and solvent deuterium isotope effects as a probe of the reaction catalyzed by porcine recombinant dihydropyrimidine dehydrogenase. Biochemistry 37 (1998) 9156-9159.
[24] M. Hedayati, B. Abubaker-Sharif, M. Khattab, A. Razavi, I. Mohammed, A. Nejad, M. Wabler, H. Zhou, J. Mihalic, C. Gruettner, T. DeWeese, R. Ivkov, An optimised spectrophotometric assay for convenient and accurate quantitation of intracellular iron from iron oxide nanoparticles. Int J Hyperthermia 34 (2018) 373-381.
[25] F.E. Smith, J. Herbert, J. Gaudin, D.J. Hennessy, G.R. Reid, Serum iron determination using ferene triazine. Clin Biochem 17 (1984) 306-310.
[26] D.J. Porter, W.G. Chestnut, B.M. Merrill, T. Spector, Mechanism-based inactivation of dihydropyrimidine dehydrogenase by 5-ethynyluracil. J Biol Chem 267 (1992) 5236-5242.
[27] D.J. Porter, T. Spector, Dihydropyrimidine dehydrogenase. Kinetic mechanism for reduction of uracil by NADPH. J Biol Chem 268 (1993) 19321-19327.
[28] W.R. Hagen, M.A. Vanoni, K. Rosenbaum, K.D. Schnackerz, On the iron-sulfur clusters in the complex redox enzyme dihydropyrimidine dehydrogenase. Eur J Biochem 267 (2000) 3640-3646.
[29] H. Beinert, R.H. Holm, E. Munck, Iron-sulfur clusters: nature's modular, multipurpose structures. Science 277 (1997) 653-659.
[30] W.V. Sweeney, J.C. Rabinowitz, Proteins containing 4Fe-4S clusters: an overview. Annu Rev Biochem 49 (1980) 139-161.
[31] D.J. Porter, Dehalogenating and NADPH-modifying activities of dihydropyrimidine dehydrogenase. J Biol Chem 269 (1994) 24177-24182.

[32] J.B. Broderick, B.R. Duffus, K.S. Duschene, E.M. Shepard, Radical S-adenosylmethionine enzymes. Chem Rev 114 (2014) 4229-4317.
[33] M.K. Bruska, M.T. Stiebritz, M. Reiher, Analysis of differences in oxygen sensitivity of Fe-S clusters. Dalton Trans 42 (2013) 8729-8735.
[34] A. Sirko, M. Zatyka, E. Sadowy, D. Hulanicka, Sulfate and thiosulfate transport in Escherichia coli K-12: evidence for a functional overlapping of sulfate- and thiosulfate-binding proteins. J Bacteriol 177 (1995) 4134-4136.
[35] V. Braun, Iron uptake by Escherichia coli. Front Biosci 8 (2003) s1409-1421.
[36] U. Schmitt, K. Jahnke, K. Rosenbaum, P.F. Cook, K.D. Schnackerz, Purification and characterization of dihydropyrimidine dehydrogenase from Alcaligenes eutrophus. Arch Biochem Biophys 332 (1996) 175-182.

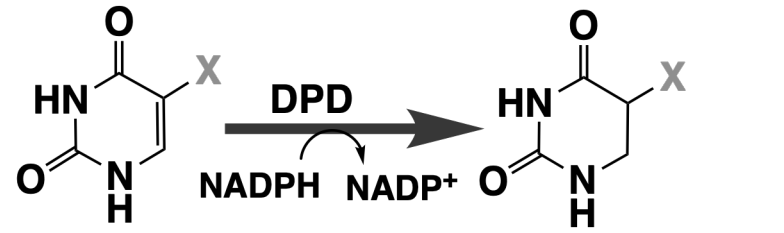

Pyrimidine Dihydropyrimidine

X = H, CH_3, F, I

SCHEME 1

	Units of Activity (DPD specific µMoles/min)					
Prep conditions	SSN	35% SN	55% pellet	Q	SEC	yield (mg)
Original protocol	5.1	3.5	3.2	3.4	3.2	9
Addition of Fe(II) and SO_4	6.8	6	4.4	4.1	3.9	11
Addition of Fe(II), SO_4, FAD, FMN	22	17	16.4	15.6	13.4	41

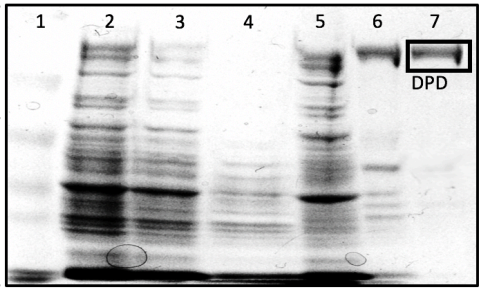

Table 1 – Total units of DPD activity for each stage of purification. The Coomasie blue stained SDS-PAGE at right summarizes the purification protocol. The loading is proportional to the sample volume at each purification stage. Lane 1 is the protein molecular weight marker (198, 62, 49, 38, 28, 18 KDa), lane 2 is the sonicate supernatant, lane 3 is the 35% ammonium sulfate supernatant, lane 4 is 55% ammonium sulfate supernatant, lane 5 is the re-dissolved 55% ammonium sulfate pellet, lane 6 is the pooled Q-sepharose sample, and Lane 7 is the pooled SEC sample. The band correlating to DPD (~113 Kda) identified by a black rectangle. The abbreviations used in the table as as follows, SSN – sonicate supernatant, 35% SN – 35% ammonium sulfate supernatant, 55% SN – 55% ammonium sulfate supernatant, Q- Q-sepharose chromatography pool, SEC- size exclusion chromatography pool.

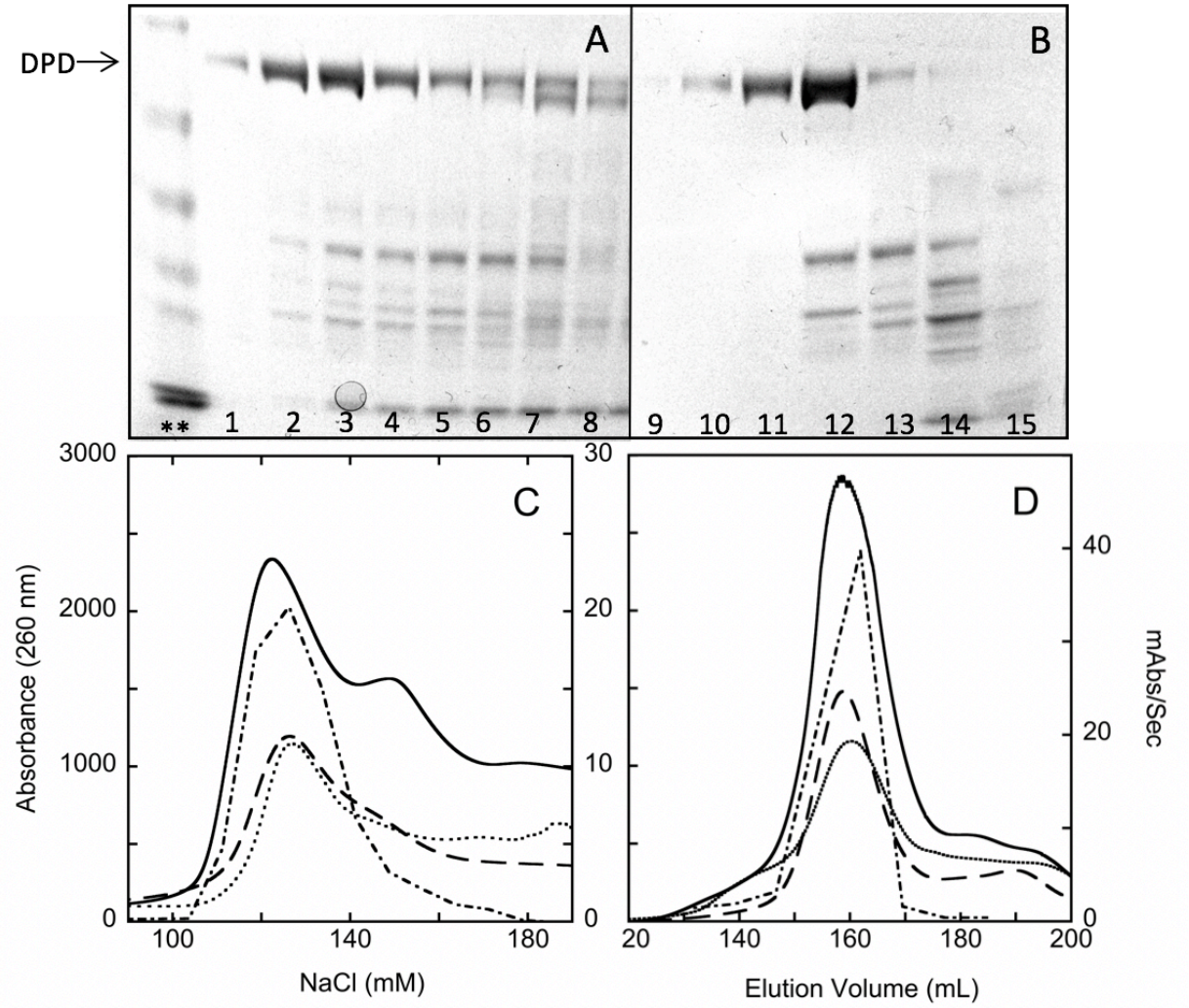

Figure 1. Analysis of DPD Purification **A**. Coomasie blue stained SDS-PAGE gel for fraction from the Q-sepharose chromatography step. Lane 1-8 are for fractions 20, 22, 24, 26, 28, 30, 32, and 34. ** is the protein molecular weight marker (198, 62, 49, 38, 28, 18 KDa) **B**. Coomasie blue stained SDS-PAGE gels of SEC fractions. Lane 9 -15 are for fractions 8, 10, 12, 14, 16, 18, and 20. **C**. & **D**. Overlay of Q-sepharose (C) and SEC (D) elution chromatograms (280 nm) for DPD from different expression protocols with per fraction DPD activity. The (⋯⋯), (– – –) and (—) are chromatograms obtained by following the original, iron sulfate supplemented and iron sulfate and flavin supplemented protocols, respectively. The (-·-) line represents activity specific to DPD in mAbs/sec for the iron sulfate and flavin supplemented protocol.

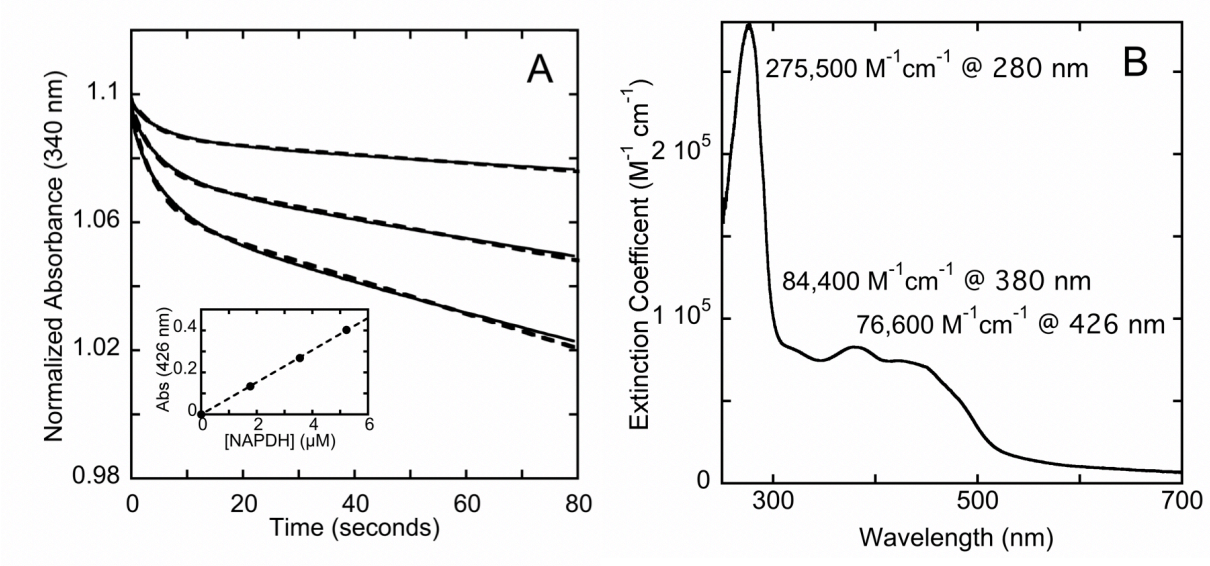

Figure 2. Determination of Active Enzyme by 5EU Inactivation. **A**. Kinetic traces in the presence of 5EU (100 µM) and NADPH (200 µM) monitoring the consumption of NADPH at 340 nm. **B**. UV-vis absorbance spectrum of DPD normalized to the extinction coefficients of DPD determined from the slope determined in A. (inset).

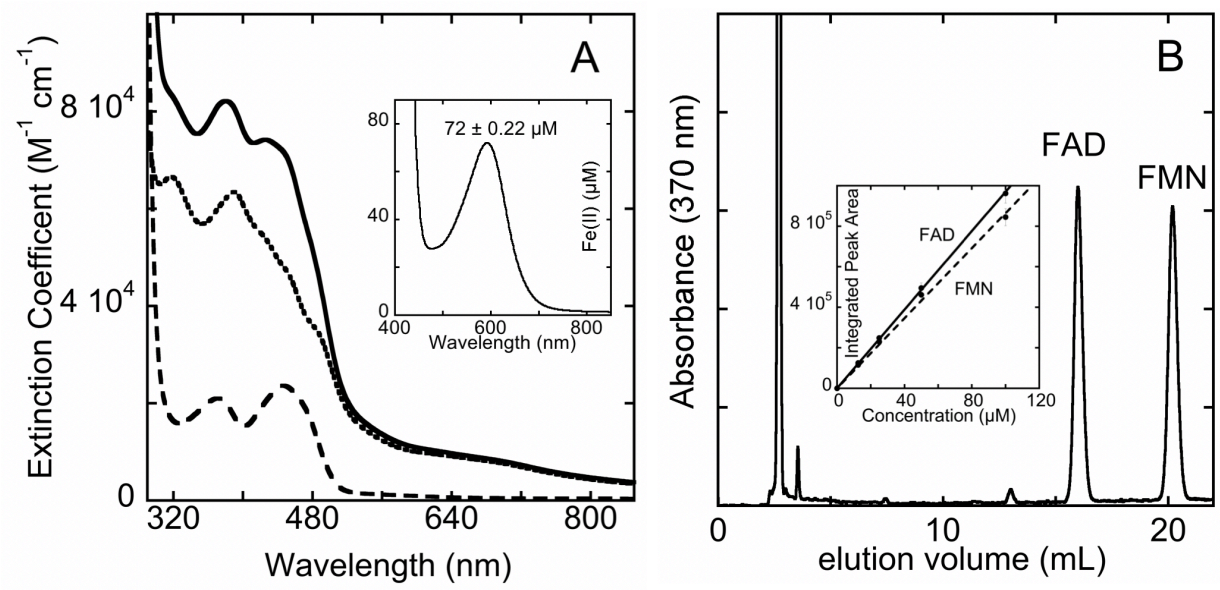

Figure 3. Analysis of DPD Cofactor Occupancy. **A**. Absorption spectrum of DPD before (—) and after (- - -) treatment of 0.2% SDS, 3mM EDTA and incubate for 1 hour at 70°C. The third spectrum (- - -) is the difference the other spectra. Absorption spectra were normalized to the 426 nm extinction coefficient of DPD (74,220 $M^{-1}cm^{-1}$). **A** inset is the absorption spectrum of DPD denatured in the presence of ferene-S and L-ascorbate. **B**. Chromatogram of UV-HPLC traces of FAD and FMN from denatured DPD. HPLC conditions: 5 mM ammonium acetate, 15% MeOH at 1 mL /minute. **B** inset is a plot of the integrated area of the HPLC peaks of FMN (- - -) and FAD (—) recorded at 370 nm.

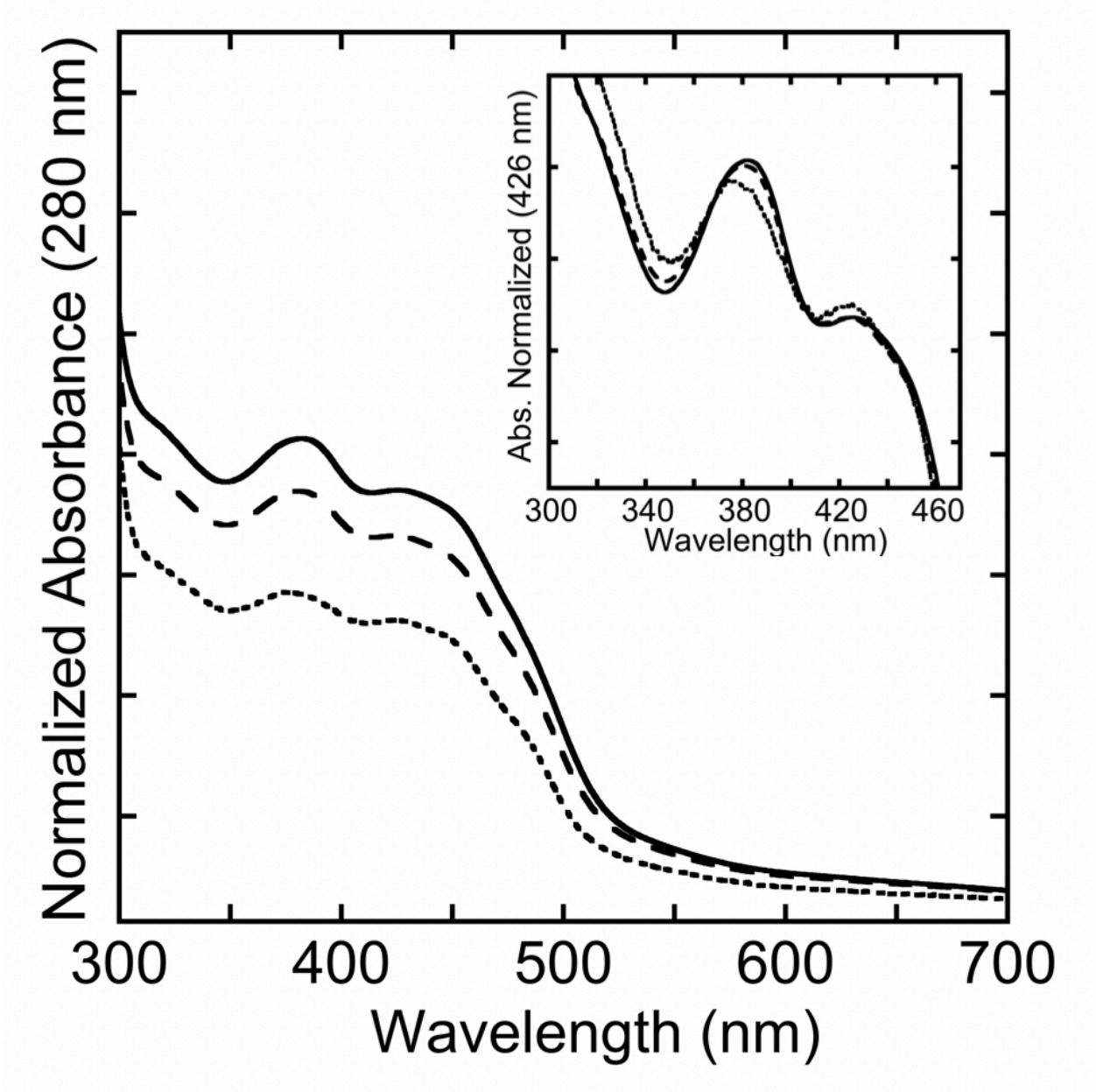

Figure 4. Absorption Spectra of DPD Expressed and Purified by Different Protocols. The spectra are representative of DPD obtained following the unsupplemented (⋯⋯), Fe (II) and sulfate supplemented (- - -) and Fe (II), sulfate and flavin supplemented (——) protocols. Spectra are normalized to 280 nm. The inset depicts the same spectra normalized at 426 nm.